Involvement of φ29 DNA polymerase thumb subdomain in the proper coordination of synthesis and degradation during DNA replication

Patricia Pérez-Arnaiz, José M. Lázaro, Margarita Salas* and Miguel de Vega

Instituto de Biología Molecular 'Eladio Viñuela' (CSIC), Centro de Biología Molecular 'Severo Ochoa' (CSIC-UAM), Universidad Autónoma, Canto Blanco, 28049 Madrid, Spain

ABSTRACT

φ29 DNA polymerase achieves a functional coupling between its 3′–5′ exonuclease and polymerization activities by means of important contacts with the DNA at both active sites. The placement and orientation of residues Lys538, Lys555, Lys557, Gln560, Thr571, Thr573 and Lys575 in a modelled φ29 DNA polymerase–DNA complex suggest a DNA-binding role. In addition, crystal structure of φ29 DNA polymerase–oligo (dT)$_5$ complex showed Leu567, placed at the tip of the thumb subdomain, lying between the two 3′-terminal bases at the exonuclease site. Single replacement of these φ29 DNA polymerase residues by alanine was made, and mutant derivatives were overproduced and purified to homogeneity. The results obtained in the assay of their synthetic and degradative activities, as well as their coordination, allow us to propose: (1) a primer-terminus stabilization role at the polymerase active site for residues Lys538, Thr573 and Lys575, (2) a primer-terminus stabilization role at the exonuclease active site for residues Leu567 and Lys555 and (3) a primer-terminus binding role in both editing and polymerization modes for residue Gln560. The results presented here lead us to propose φ29 DNA polymerase thumb as the main subdomain responsible for the coordination of polymerization and exonuclease activities.

INTRODUCTION

Proper transmission of genetic information from one generation to the next requires the synthesis of a faithful copy of the genome during the DNA replication process. Although several postreplicative mechanisms have evolved to guarantee the maintenance of such information, as those responsible of repairing DNA damages produced by cellular metabolism and exogenous genotoxicans (1) as well as those involved in correcting the polymerization errors that escape proof-reading (1,2), replicative DNA polymerases are the major enzymes responsible for the exceptional fidelity exhibited by most organisms in performing that task, inserting only 10^{-5}–10^{-8} errors per nucleotide (3,4). The significant precision of DNA synthesis by these DNA polymerases resides in the acquisition of two fidelity devices: (1) base selection, by which DNA polymerases discriminate between correct and incorrect nucleotides in the polymerization step by virtue of the stringent exigency for the precise geometry of the Watson and Crick base pair, showing error rates for single-base substitutions varying from 10^{-3} to >10^{-6} (5); (2) a proofreading mechanism, dependent on a 3′–5′ exonuclease activity which is physically associated with the DNA polymerase, both acting in a coordinated manner to remove preferentially non-complementary nucleotides at the 3′ end of primer molecules, increasing base substitution fidelity from a few fold to >100-fold (5).

Replicative DNA polymerases whose structure has been solved show a common folding pattern, with a C-terminal domain containing the catalytic residues involved in polymerization, and structured as a partially open right hand with the universal palm, thumb and fingers subdomains that form a U-shaped groove to allocate the primer–template DNA (6–12). In addition, most of them also contain a 3′–5′ exonuclease domain with the catalytic residues involved in proofreading of the misinserted nucleotides. The separation between both polymerization and 3′–5′ exonuclease active sites (30–40 Å), allows a fine-tuned coordination of these opposite activities to permit a productive and faithful DNA synthesis, being required a functional communication between the two active sites during polymerization to permit the elimination of only the misinserted nucleotide without compromising the energetics of the process (elimination of correct nucleotides) or the polymerization progress.

Structural resolution of DNA polymerases complexed with a DNA substrate has given insights about the principles that govern the transference of the 3′ terminus between both active sites (6,7,9,12). Briefly, once a nucleotide is misinserted, the mismatched primer-terminus cannot attack

*To whom correspondence should be addressed. Tel: +34 91 4978435; Fax: +34 91 4978490; Email: msalas@cbm.uam.es

nucleophylically the next incoming nucleotide, avoiding further polymerization reactions. In addition, the mispair breaks interactions with minor groove hydrogen bond acceptors at the polymerization active site, increasing the probability of the primer-terminus switching to the exonuclease site, guided by the thumb subdomain (12).

Bacteriophage φ29 has a protein-primed DNA polymerase belonging to the eukaryotic-type family of DNA polymerases (family B) being the only enzyme responsible of the viral genome replication (13,14). It shows three differential characteristics: (1) it initiates DNA replication using a terminal protein (TP) as primer, inserting the first dAMP onto the hydroxyl group of Ser^{232} of TP (13,14); (2) unlike most replicases, φ29 DNA polymerase couples DNA polymerization to strand displacement, precluding the assistance by DNA unwinding factors (15); (3) contrary to most replicases, φ29 DNA polymerase performs viral DNA replication without the need of processivity factors, being, to our knowledge, the most processive DNA polymerase described (15). Additionally, it also contains a 3′–5′ exonuclease activity involved in editing the misinserted nucleotides during polymerization (16). The biochemical properties of φ29 DNA polymerase, high processivity and strand displacement capacity, impose a tight functional communication between both polymerization and exonuclease active sites. The equilibrium between synthesis and degradation depends on the relative catalytic rates (17,18) and on the strength of the primer-terminus binding to both active sites, as demonstrated by extensive site-directed mutagenesis studies (14,17,18).

Recent crystallographic determination of φ29 DNA polymerase structure shows how the enzyme presents the common folding described above, with a C-terminal domain having the polymerization active site and an N-terminal one containing the 3′–5′ exonuclease active site, both domains oriented to each other as in the other crystallized family B DNA polymerases (19). In addition to the palm, fingers and thumb subdomains, the polymerization domain of φ29 DNA polymerase presents two additional subdomains, both corresponding to sequence insertions specifically conserved in the protein-primed DNA polymerases, and called TPR1 and TPR2, the last one involved in conferring both processivity and strand displacement capacity to the DNA polymerase by closing completely the universal DNA-binding groove at the polymerization active site (19,20).

In this study we describe the central role of φ29 DNA polymerase thumb subdomain in coordinating both polymerization and exonuclease activities due to the presence of DNA ligands specialized in binding the DNA substrate either at one or both active sites.

MATERIALS AND METHODS

Nucleotides and DNAs

Unlabelled nucleotides were purchased from Amersham Pharmacia Biochemicals. [γ-^{32}P]dATP [3000 Ci/mmol (1 Ci = 37 GBq)] and [γ-^{32}P]ATP (3000 Ci/mmol) were obtained from Amersham Pharmacia. Oligonucleotide sp1 (5′-GATCACAGTGAGTAC) was 5′-labelled with [γ-^{32}P] ATP and phage T4 polynucleotide kinase and purified electrophoretically on 8 M urea/20% polyacrylamide gels.

Labelled sp1 was hybridized to oligonucleotide sp1c + 6 (5′-TCTATTGTACTCACTGTGATC) in the presence of 0.2 M NaCl and 50 mM Tris–HCl (pH 7.5), resulting in a primer–template structure. Oligonucleotides sp1 and sp1c + 6 were obtained from Isogen. To analyse processive DNA polymerization coupled to strand displacement by φ29 DNA polymerase, M13mp18 single-stranded DNA (ssDNA) was hybridized to the universal primer (Isogen) in the presence of 0.2 M NaCl and 60 mM Tris–HCl (pH 7.5). TP-containing φ29 DNA (φ29 TP-DNA) was obtained as described (21).

Proteins

Phage T4 polynucleotide kinase was obtained from New England Biolabs. Wild-type φ29 DNA polymerase was purified from *Escherichia coli* NF2690 cells harbouring plasmid pJLPM (a derivate of pT7-4w2), as described (22). The φ29 DNA polymerase mutants were purified essentially in a similar way, from *E.coli* BL21(DE3) cells harbouring the corresponding recombinant plasmid. φ29 TP was purified as described (23).

Site-directed mutagenesis of φ29 DNA polymerase

φ29 DNA polymerase mutants (K538A, K555A, K557A, Q560A, L567A, T571A, T573A and K575A) were obtained by using the QuickChange site-directed mutagenesis kit provided by Amersham Pharmacia. Plasmid pJLPM containing the φ29 DNA polymerase gene was used as template for the mutagenesis reaction. After temperature cycling using PfuTurbo DNA polymerase and treatment with DpnI endonuclease, synthesized DNA was transformed into XL1-blue supercompetent cells. The presence of the desired mutation and absence of other mutations were confirmed by sequencing the entire gene.

3′–5′ Exonuclease assay

The incubation mixture contained, in a final volume of 12.5 µl, 50 mM Tris–HCl (pH 7.5), 1 mM DTT, 4% glycerol, 0.1 mg/ml BSA and 10 mM MgCl$_2$. As substrate, 1.2 nM of 5′-labelled sp1 (ssDNA) or 1.2 nM of the hybrid molecule sp1/sp1c + 6 double-stranded DNA (dsDNA) was used. The amount of DNA polymerase added (6 nM) was adjusted to obtain linear conditions. Samples were incubated at 25°C for the indicated times and quenched by adding 3 µl of gel loading buffer. Reactions were analysed by electrophoresis in 8 M urea/20% polyacrylamide gels and densitometry of the autoradiograph. Total degradation was obtained by calculating the number of catalytic events giving rise to each degradation product. From these data, the catalytic efficiency of each mutant derivate (indicated in Table 1) was calculated relative to wild-type φ29 DNA polymerase.

Polymerase/3′–5′ exonuclease (pol/exo) coupled assay

The DNA molecule sp1/sp1c + 6 (15mer/21mer) contains a 6 nt 5′-protruding end and can therefore be used as substrate for the exonuclease activity (dsDNA) and also for DNA-dependent DNA polymerization. The incubation mixture contained, in 12.5 µl, 50 mM Tris–HCl (pH 7.5), 10 mM MgCl$_2$, 1 mM DTT, 4% (v/v) glycerol, 0.1 mg/ml BSA, 1.2 nM of 5′-labelled 15/21mer, 30.3 nM of wild-type or mutant

Table 1. Enzymatic activities of wild-type and mutant derivatives of φ29 DNA polymerase

Activity assay	Substrate(s)	φ29 DNA polymerase[a]								
		wt	K538A	K555A	K557A	Q560A	L567A	T571A	T573A	K575A
3′–5′ Exonuclease	ssDNA (spl)	100	164	77	73	22	14	68	67	88
	dsDNA (spl/spl c + 6)	100	264	44	82	49	9	157	115	164
Pol/Exo balance[b]	spl/spl c + 6, dNTP	25/50	1000	25	25/50	25/50	615	25/50	1000	100/200
Stable DNA binding { Pol[c]	spl/spl c + 6	100	<2	80	23	13	45	110	6	55
Exo[d]	spl/spl c + 6	100	155	110	75	7	3	144	72	79

[a]Numbers indicate the average percentage of activity relative to the wild-type enzyme obtained from several experiments.
[b]Numbers indicate the dNTP concentration (in nM) required to efficiently elongate the 15mer primer until the 20mer position.
[c]Stabilization of the primer-terminus at the polymerization active site, as defined by gel retardation of a template/primer structure.
[d]Stabilization of the primer-terminus at the 3′-5′ exonuclease active site, as defined by gel retardation assay of ssDNA.

φ29 DNA polymerases and the indicated increasing concentrations of the four dNTPs. After incubation for 10 min at 25°C, the reaction was stopped by adding EDTA up to a final concentration of 10 mM. Samples were analysed by electrophoresis in 8 M urea/20% polyacrylamide gels and autoradiography. Polymerization or 3′–5′ exonucleolysis is detected as an increase or decrease, respectively, in the size (15mer) of the 5′-labelled primer.

Misincorporation assay

Conditions were essentially as described above for the polymerization/exonuclease coupled assay on sp1/sp1c + 6, but in this case, increasing concentrations of only dATP, complementary to positions 1, 2, 4 and 6 was added. To prevent exonucleolytic degradation of the primer-terminus, 25 μM dCTP was added. After incubation for 5 min at 30°C, samples were analysed by 8 M urea/20% polyacrylamide gel electrophoresis. After autoradiography, misinsertion of dAMP at non-complementary positions is observed as the appearance of extension products of the 5′-labelled sp1 primer (15mer), larger than the correct 17mer extension product. The misincorporation produced in each case, expressed as the ratio 18mer + 19mer/17mer + 18mer + 19mer, was determined by densitometry of the autoradiogram.

DNA gel retardation assay

The interactions of either the wild-type or the φ29 DNA polymerase mutants with the primer–template structure was assayed using the 5′-labelled sp1/sp1c + 6 (15/21mer) DNA. The incubation mixture contained, in a final volume of 20 μl, 12 mM Tris–HCl (pH 7.5), 1 mM EDTA, 20 mM ammonium sulphate, 0.1 mg/ml BSA, 10 mM MgCl₂, 0.7 nM of sp1/sp1c + 6 and 1.9 nM of wild-type or mutant φ29 DNA polymerases. The binding to ssDNA was assayed under the same conditions described above, in the absence of MgCl₂, using 1.4 nM sp1 and 0.5 nM of wild-type or mutant φ29 DNA polymerases. After incubation for 5 min at 4°C, the samples were subjected to electrophoresis in precooled 4% (w/v) polyacrylamide gels (80:1, monomer:bis) containing 12 mM Tris–acetate (pH 7.5) and 1 mM EDTA, and run at 4°C in the same buffer at 8 V/cm (24). After autoradiography, φ29 DNA polymerase/DNA stable interaction was detected as a shift (retardation) in the migrating position of the labelled DNA, and quantified by densitometry of the autoradiograms corresponding to different experiments.

RESULTS

Putative DNA ligand residues of the thumb subdomain of φ29 DNA polymerase

Recent crystallographic resolution of φ29 DNA polymerase structure shows how the TPR2 insertion, specifically present in the protein-primed DNA polymerases subgroup, generates the formation of two electropositively charged paths leading into the active site of φ29 DNA polymerase (19). One of them is participated also by residues from the exonuclease domain and fingers and palm subdomains, that form a downstream tunnel through which the template strand is threaded, this being the structural basis of the strand displacement capacity of the φ29 DNA polymerase [(19,20); see also Figure 1A]. Residues from the palm, thumb, TPR1 and TPR2 subdomains surround a second tunnel (upstream duplex tunnel) into the φ29 DNA polymerase active site encircling a homology-modelled upstream duplex DNA (19) conferring processivity to the DNA polymerase (20). By superimposing the palm subdomains of both φ29 and RB69 DNA polymerases, we have modelled the DNA of the RB69 ternary complex onto the structure of apo φ29 DNA polymerase, the location of the catalytic and DNA-binding residues being consistent with the position and orientation of the modelled DNA, as described (19). A detailed examination of the modelled complex between the DNA polymerase and the DNA shows the presence of the electropositive and polar residues Lys538, Lys555, Lys557, Gln560, Thr571, Thr573 and Lys575 from the unusually structured thumb subdomain (mainly made of a loop and a long β-turn-β element) placed close enough to make contacts with the DNA through its minor groove (Figure 1B). With the exception of residue Lys538, the rest of them belong to the β-turn-β element of such a subdomain [(19); and figures therein]. As shown in Figure 1B, these residues can be grouped into two clusters. Lys538, Lys555, Lys557 and Gln560 would be placed following the path of the primer-terminus, while Thr571, Thr573 and Lys575 would follow the template strand contour close to the catalytic site, suggesting a functional division of φ29 DNA polymerase thumb residues. Their placement, together with the fact that a deletion of the C-terminal 13 residues of φ29 DNA polymerase strongly affected DNA-binding (25), lead us to propose them as putative DNA ligands at the polymerization active site of the polymerase. In addition, co-crystals of φ29 DNA polymerase with a bound (dT)₅ oligonucleotide at its 3′–5′ exonuclease active site show how residue Leu567, also belonging to the thumb subdomain, lies between and
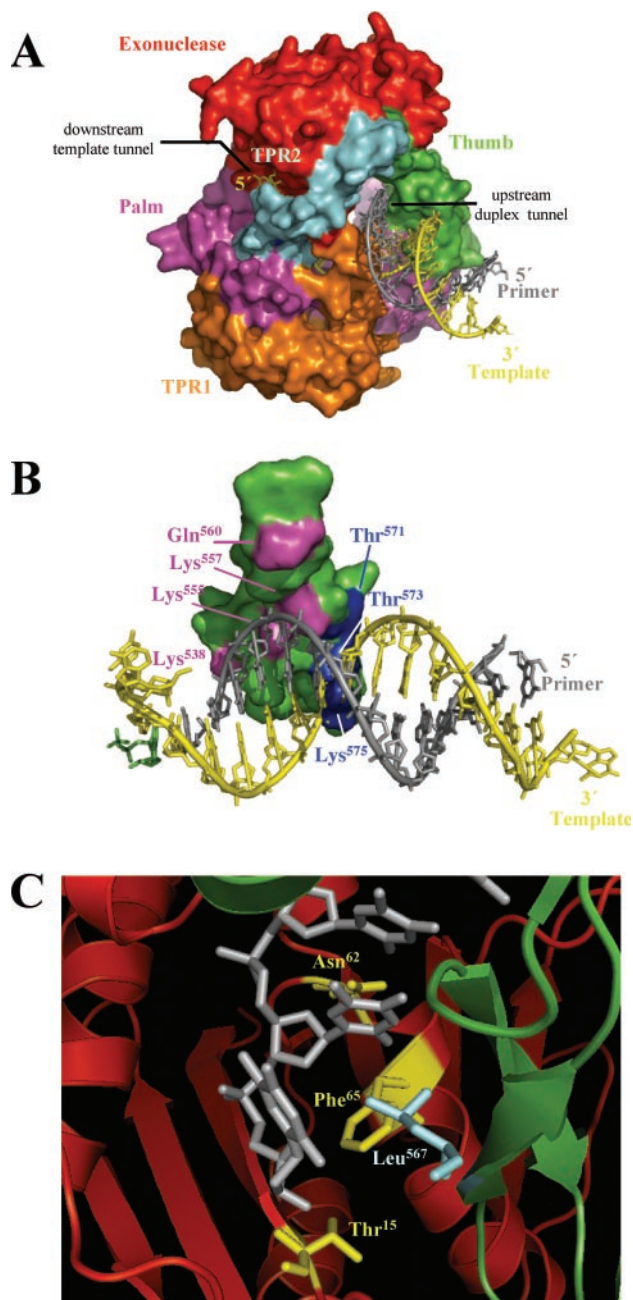
Figure 1. φ29 DNA polymerase thumb subdomain. (**A**) Modelling of φ29 DNA polymerase interaction with duplex DNA. φ29 DNA polymerase is space filling represented, and coloured as in (19). DNA from the structure of RB69 ternary complex (12) is modelled onto the structure of φ29 DNA polymerase, as described (19). Crystallographic data are from Protein Data Bank ID codes 1XHX (φ29 DNA polymerase) and 1 IG9 (RB69 DNA polymerase ternary complex). (**B**) φ29 DNA polymerase thumb subdomain interacts with the DNA minor groove. Detailed picture showing the proposed φ29 DNA polymerase residues acting as DNA ligands. Those residues proposed to interact with the primer strand are coloured in magenta while those proposed to interact with the template strand are coloured in dark blue. The incoming nucleotide is coloured in green. (**C**) Stabilization of ssDNA at φ29 DNA polymerase 3′–5′ exonuclease active site. Residues proposed to be involved in primer-terminus stabilization at the exonuclease site of φ29 DNA polymerase, and belonging to the Exo I and Exo II motifs of the exonuclease domain are coloured in yellow (26,27). Leu567 from the thumb subdomain, proposed to be interacting with the two 3′-terminal nucleotides of the primer-terminus at the exonuclease site (19), is coloured in blue. Figure was made using Pymol (http://www.pymol.org)

interacts with the two 3′-terminal bases, suggesting a role in the proper stabilization of the primer-terminus at this catalytic site [(19); Figure 1C], and hence, in the coordination between the synthetic and degradative activities. The very low sequence similarity and length heterogeneity among the thumb subdomain of DNA polymerases do not allow to find a multiple alignment of such a region of the enzyme, leading us to restrict it to the protein-priming subgroup of family B DNA polymerases. Based on this alignment, we found that residues corresponding to φ29 DNA polymerase Lys555 and Lys575 are conserved in most of the subgroup members, while residues homologous to Lys538, Lys557, Gln560, Leu567 and Thr573 of φ29 DNA polymerase were restricted to DNA polymerases from φ29-related phages.

To analyse their functional role, we substituted the side chain of all the above-mentioned residues to alanine, removing the positive charge in the case of lysines, the polar group of the threonines and glutamine, and shortening the aliphatic side chain of the leucine residue. All the mutations introduced were predicted to maintain the overall structure in that region of the polypeptide. The mutant derivatives were overexpressed and purified as described in Materials and Methods, their catalytic activities being analysed by *in vitro* assessment.

3′–5′ Exonuclease activity of φ29 DNA polymerase mutants

Based on the crystallographic structure of φ29 DNA polymerase, the residues mutated, except Leu567, are far away from the 3′–5′ exonuclease active site, not playing, a priori, any direct role in the exonuclease activity of the DNA polymerase (19). From an enzymatic point of view, the optimal substrate for the 3′–5′ exonuclease activity of DNA polymerases is ssDNA. To measure the capacity of mutant polymerases to degrade this kind of molecules, sp1 oligonucleotide was used as substrate of their 3′–5′ exonuclease activity (see Materials and Methods). As shown in Figure 2, the wild-type enzyme is able to degrade the oligonucleotide sp1
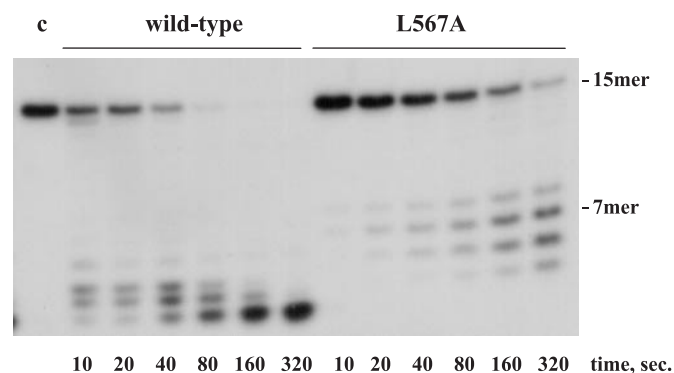

Figure 2. φ29 DNA polymerase mutant L567A displays a defective 3′–5′ exonuclease activity on ssDNA. The assay was performed as described in Materials and Methods, using ^{32}P-labelled sp1 as ssDNA substrate. After incubation for the indicated times at 25°C, degradation of the labelled DNA was analysed by electrophoresis in 8 M urea/20% polyacrylamide gels and autoradiography. Total degradation was calculated as indicated in Materials and Methods. The position of different degradation intermediates of the sp1 substrate (15mer) is indicated.

in a processive way until the length is shortened to a 5/6mer, further degradation from this position being distributive. With the exception of mutant L567A, the rest of the protein derivatives showed a similar degradation pattern (data not shown) with global degradation efficiency higher (K538A), similar (K555A, K557A, T571A, T573A and K575A) or lower (Q560A and L567A) than that of the wild-type enzyme (see Table 1). Mutant L567A displayed a degradation pattern significantly different, showing a preferential stop in the 6/7mer position (see Figure 2), not being able to reach lengths shorter than 5mer at longer reaction times. This fact states the importance of Leu567 as ssDNA ligand at the 3′–5′ exonuclease active site, its role being more critical with short substrates, conditions under which the enzyme–DNA interactions are mainly dependent on specific contacts through DNA ligands placed close to the active site (26,27). Interestingly, when a more physiological substrate of the 3′–5′ exonuclease was used (duplex sp1/sp1c + 6; see Materials and Methods), the activity displayed by mutants K538A, Q560A, T571A, T573A and K575A was higher than when ssDNA was used (see Table 1). Under such conditions there is a competition between two primer-terminus binding modes: for exonucleolytic degradation, binding at the 3′–5′ exonuclease active site should outcompete the binding strength at the polymerization active site, which is contributed by specific DNA ligand residues and by Watson and Crick pairing. The results mentioned above suggest a defective binding of the primer-terminus at the polymerization active site of mutants K538A, Q560A, T571A, T573A and K575A, favouring the exonucleolytic degradation of the dsDNA substrate, in comparison to ssDNA. Conversely, mutant K555A exhibited a lower exonuclease activity on dsDNA than on ssDNA.

Exonucleolysis to polymerization switching of φ29 DNA polymerase mutants

As most replicases, the exonuclease and polymerization activities of φ29 DNA polymerase reside in two structurally independent domains of the same polypeptide chain, the C-terminal one containing the polymerization active site whereas the smaller N-terminal domain contains that for the 3′–5′ exonuclease activity (17–19). In spite of their structural separation, both active sites must work in concert to ensure a productive and faithful DNA synthesis, preventing the accumulation of errors in the newly synthesized strand while allowing a proper elongation rate. The decision to synthesize versus to degrade the primer-terminus will depend on several factors, as the relative velocity of both activities and the comparative stabilization of the primer-terminus at such active sites.

To evaluate how the mutations introduced affected the dynamic equilibrium between the 3′–5′ exonuclease and 5′–3′ polymerization activities of φ29 DNA polymerase, we studied the functional coupling between synthesis and degradation on a primer–template hybrid molecule (sp1/sp1c + 6) as a function of dNTP concentration (see Materials and Methods). In the absence of nucleotides, the only bands that could be detected corresponded to primer degradation products due to the 3′–5′ exonuclease activity (see Figure 3). As the concentration of the unlabelled dNTP provided was increased, this activity was progressively competed by the 5′–3′ polymerization, and net dNTP incorporation was observed as an increase in the size of the labelled primer, allowing us to define a dNTP concentration to obtain an efficient elongation for each mutant derivative. As shown in Table 1, the Pol/Exo ratio of mutants K557A, Q560A and T571A was similar to that of the wild-type enzyme, requiring 25–50 nM dNTPs to elongate the primer efficiently. However, mutant proteins K538A, T573A and K575A required a dNTP concentration >20- (in the case of the two formers) and 4-fold (in the case of the last) higher than that of the wild-type enzyme (see Table 1 and Figure 3) showing a strong 3′–5′ exonuclease activity on duplex DNA. The poor polymerization activity displayed by these mutant derivatives under the Pol/Exo assay conditions could be a direct consequence of a defective binding of the primer-terminus at the polymerization active site (as described above) resulting
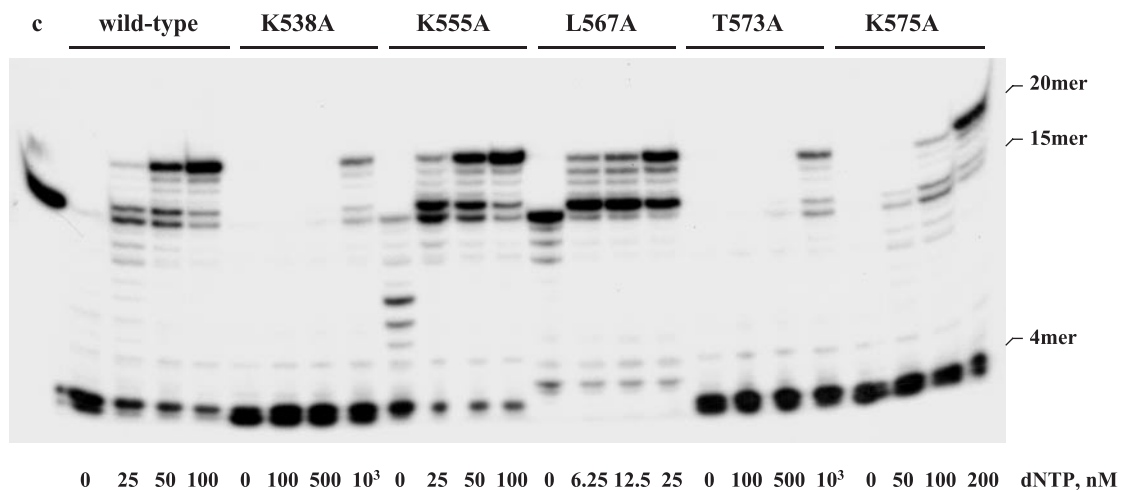

Figure 3. DNA polymerase/exonuclease coupled assay. The assay was carried out as described under 'Materials and Methods' using ^{32}P-labelled sp1/sp1c + 6 as primer–template DNA and the indicated concentration of each dNTP. Polymerization or 3′–5′ exonuclease activity is detected as an increase or decrease, respectively, in the size (15mer) of the 5′-labelled primer. The productive Pol/Exo ratio and the relative polymerization for each mutant polymerase are indicated in Table 1.

in the increased exonuclease activity on dsDNA indicated before. Considering the wild-type Pol/Exo ratio displayed by mutant T571A, its high exonuclease activity on dsDNA (described above) cannot be justified by a defective DNA interaction at the polymerization active site, as suggested in the previous section, but by a stable DNA polymerase–DNA complex. Conversely, the dNTP concentration required by mutant L567A was 4-fold lower than that of the wild-type polymerase. This could be explained by its defective 3′–5′ exonuclease activity, as a direct consequence of its impaired binding of the primer-terminus at the exonuclease active site (see above). The 2-fold lower amount of nucleotides required by mutant K555A to get a productive elongation compared to the wild-type enzyme is in accordance to its reduced 3′–5′ exonuclease activity on dsDNA, suggesting a secondary role in the exonucleolytic degradation of the primer-terminus.

The high Pol/Exo ratio displayed by mutant L567A and to a lower extent, by mutant K555A, led us to analyse whether these derivatives were able to produce a stable incorporation of incorrect nucleotides during polymerization. To address this question, we performed a misincorporation assay (see Materials and Methods), analyzing the insertion of dAMP by mutant polymerases at non-complementary positions, in comparison with the wild-type enzyme and the φ29 DNA polymerase 3′–5′ exonuclease defective mutant D12A/D66A (28). Under such conditions, the wild-type enzyme was not able to produce a stable incorporation of dAMP at the non-complementary position 18, with dAMP insertion occurring only at the complementary positions 16 and 17 (see Figure 4). Conversely, when mutant D12A/D66A was assayed, the presence of label at position 19 indicated that dAMP misincorporation and further elongation of the mismatched primer-terminus were allowed. The absence of label at position 18 indicated that nucleotide misinsertion

was the rate-limiting step. Quantification of the misincorporation produced by this mutant DNA polymerase allowed us to calculate a 24-fold reduction in fidelity with respect to the wild-type enzyme. As it can be seen in Figure 4, mutant L567A and, in a minor extent, K555A, also yielded stable misincorporation of dAMP, showing a fidelity reduction of 13- and 4-fold, respectively, relative to the wild-type DNA polymerase, in accordance with their increased Pol/Exo ratio.

Mutation at residues Lys538, Gln560 and Thr573 impairs binding of primer–template DNA molecules at the φ29 DNA polymerization active site

To analyse the capacity of mutant derivatives to efficiently bind a primer-terminus, gel shift assays were carried out, using the hybrid sp1/sp1c + 6 as substrate (see Materials and Methods). As shown in Figure 5A, the wild-type enzyme gave rise, in the presence of Mg^{2+}, to a single retardation band, which we interpreted as a stable complex in which the primer-terminus was stabilized at the polymerization active site (29). As described (30), defects in the primer stabilization at the polymerization active site would lead to a metal activated exonucleolytic degradation of the primer-terminus giving products that would migrate faster than the non-bound substrate. As also shown in Figure 5A, mutant K555A was able to retard the sp1/sp1c + 6 in a nearly wild-type fashion (see also Table 1) and, in a lower extent, mutants K557A, L567A and K575A. Conversely, mutants K538A and T573A did not give a stable retarded band, indicating serious binding defects at the polymerization active site. As a direct consequence of such a poor stabilization, most of the substrate added was degraded by their exonucleolytic activity (see Figure 5A). On the other hand, mutant Q560A gave rise to a low intense retardation band.
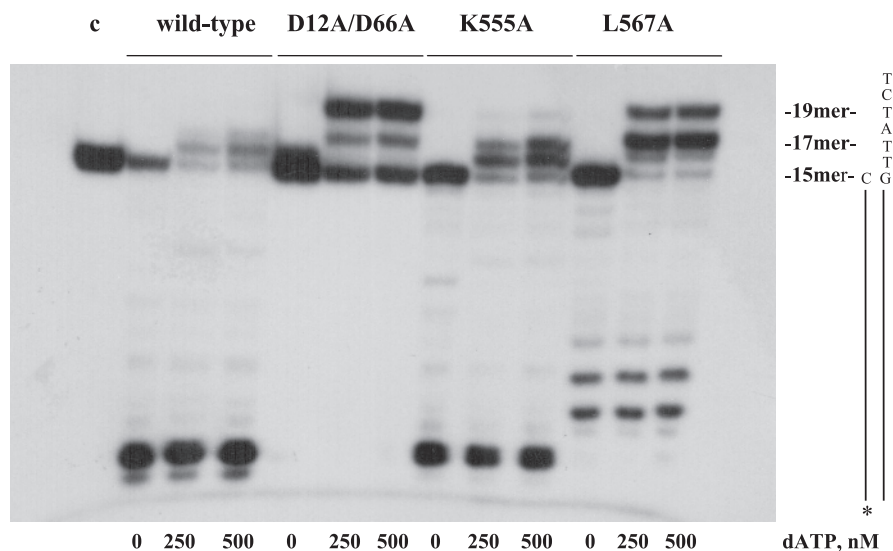

Figure 4. Misincorporation during DNA replication by mutants in residues Lys555 and Leu567 of φ29 DNA polymerase. The assay was carried out in the conditions described in Materials and Methods, using 1.2 nM of 5′-labelled hybrid sp1/sp1c + 6 (whose sequence is partially shown at the right), 30.3 nM of either wild-type or the indicated mutant DNA polymerase, and the indicated concentration of dATP. A φ29 DNA polymerase double mutant [D12A/D66A; (28)], devoid of 3′–5′ exonuclease activity, was included as a control of the maximal misincorporation frequency. After incubation for 5 min at 30°C, the reaction products were analysed by electrophoresis in 8 M urea/20% polyacrylamide gels, followed by autoradiography. The positions corresponding to the unextended primer (15mer) and to extended (17 and 19mer) products, are indicated. Relative misincorporation, calculated as the ratio 18 + 19mer/17 + 18 + 19mer is indicated in the text.
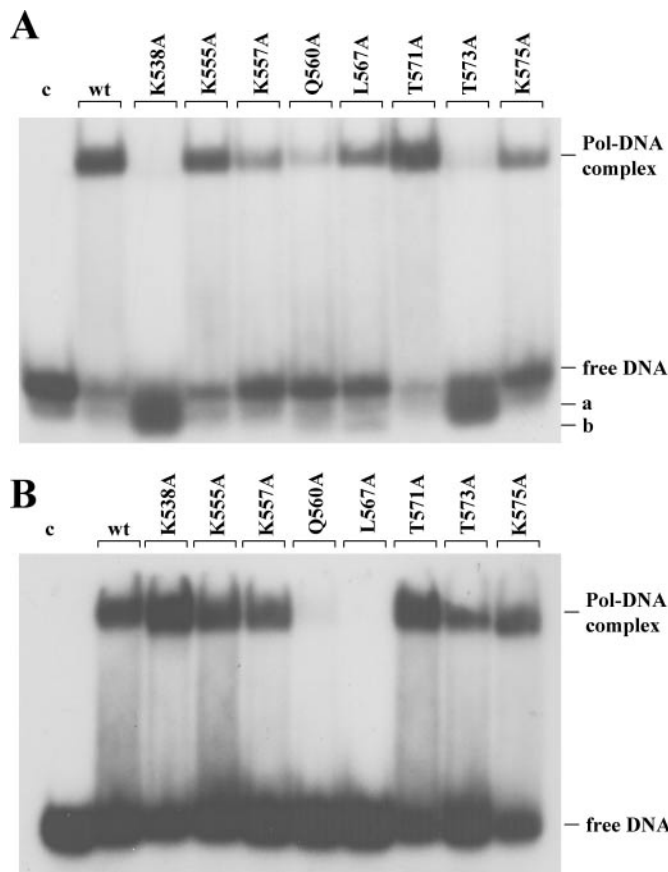
Figure 5. (**A**) Gel retardation of primer–template DNA molecules. The 5′-labelled hybrid molecule sp1/sp1c + 6 was incubated either with the wild-type or with the indicated mutant derivative, under the conditions described in Materials and Methods. After gel electrophoresis, the mobility of free DNA (sp1/sp1c + 6) and the polymerase–DNA complex was detected by autoradiography. a, unhybridized primer strand (sp1); b, degraded primers. (**B**) Gel retardation of ssDNA molecules. The 5′-labelled oligonucleotide sp1 was incubated either with the wild-type or with the indicated mutant derivative of ϕ29 DNA polymerase, under the conditions described in Materials and Methods. After gel electrophoresis, the bands corresponding to free ssDNA (sp1) and to DNA polymerase–ssDNA complex were detected by autoradiography.

Nevertheless, contrary to the above-mentioned mutants, Q560A did not exhibit an increased exonucleolytic degradation of the DNA substrate. In addition, mutant T571A showed a high dsDNA-binding stability, in accordance to its improved 3′–5′ exonuclease activity on dsDNA and its wild-type Pol/Exo ratio.

To study the binding capacity of mutant DNA polymerases for ssDNA, we evaluated their ability to retard the sp1 molecule by gel shift assays (see Materials and Methods). As shown in Figure 5B, the wild-type enzyme produced a single retardation band, most likely corresponding to a DNA polymerase–ssDNA complex in which the 3′-terminus was stably bound at the exonuclease active site (26). Mutant Q560A bound ssDNA very poorly and at a similar extent as when dsDNA was used as substrate (see above). This fact would indicate that residue Gln560 could be acting as a primer-terminus ligand in both polymerization and editing modes. Interestingly, mutant L567A was very defective in stabilizing the ssDNA at its exonuclease active site, pointing

to a specific role for residue Leu567 as primer-terminus ligand exclusively in editing DNA polymerase–DNA complexes. The rest of mutant derivatives behaved in a wild-type fashion (Figure 5B and Table 1).

DISCUSSION

Coupling between both polymerization and proofreading activities

Proofreading DNA-dependent DNA polymerases belonging to families A and B contain both 3′–5′ exonuclease and 5′–3′ polymerization active sites, spatially separated 30–40 Å (8,10,11,13,19,31). As a consequence, a very precise functional coupling of such activities to perform DNA replication in an effective and accurate way is needed, being required an efficient transfer of the 3′ terminus of the newly synthesized strand between exonuclease and polymerization sites by specialized DNA ligand residues.

The modelled DNA onto the structure of the apo ϕ29 DNA polymerase has served to identify residues Lys538, Lys555, Lys557, Gln560, Thr571, Thr573 and Lys575 placed at an electropositive region of the thumb subdomain that, due to their proximity and orientation toward the minor groove of the DNA, could be playing a role as ligands of the DNA at the polymerization active site. In addition, the co-crystal with a bound $(dT)_5$ oligonucleotide has allowed us to identify residue Leu567, also belonging to the thumb subdomain, as a putative ssDNA ligand at the 3′–5′ exonuclease active site that could be contributing to the ssDNA-binding stability during proofreading (19). We have analysed the role of the aforementioned residues by assaying the synthetic (polymerization) and degradative (3′–5′ exonuclease) activities of the corresponding mutant derivatives.

Primer-terminus stabilization at the polymerization active site of ϕ29 DNA polymerase

Biochemical analysis of ϕ29 DNA polymerase mutants K538A, T573A and K575A showed that these derivatives were provided with a higher exonuclease activity on dsDNA than on ssDNA substrates. As a result, their Pol/Exo ratios were drastically reduced, mainly in the case of mutants K538A and T573A. This was probably due to a diminished primer-terminus stability at the polymerization active site, as deduced from gel shift assays. These residues of ϕ29 DNA polymerase are placed in the base part of the thumb subdomain. Modelling of the interaction of a DNA at the polymerization site of ϕ29 DNA polymerase shows the closeness of the Lys538 side chain to the penultimate phosphodiester bond of the primer strand, most likely contributing to its stabilization at the polymerization site, in good agreement with the high exonuclease activity and the low Pol/Exo ratio displayed by mutant K538A. Conversely, residues Thr573 and Lys575 would be oriented toward and in a very close proximity to the phosphodiester bond between the sixth and seventh nucleotide of the template strand. If this were the case, it is tempting to attribute to these two residues a subtler role in the proper placement and/or orientation of the template strand at the polymerization site. Such a disturbed binding would hinder the stable insertion of an

incoming dNTP onto the growing strand due to the difficulty to form a base pair with the template dNMP.

The results presented above enlarge our knowledge about the residues involved in primer-terminus stabilization at the polymerization site of the φ29 DNA polymerase. Based on multiple amino acid sequence alignments, eleven residues, invariantly or highly conserved in the C-terminal domain of eukaryotic-type DNA polymerases (family B), were implicated in such binding. Those residues belong to (1) palm subdomain motifs 'Dx$_2$SLYP', 'Tx$_2$G/AR' and 'KxY' (14,17,18); (2) fingers subdomain motif 'KLx$_2$NSxYG' (14,17,18) and (3) TPR1 insertion (32). On the other hand, by site-directed mutagenesis of φ29 DNA polymerase, it was demonstrated that the conserved motif 'YxG(G/A)', located between the 3′–5′ exonuclease and polymerization domains of family B DNA polymerases, is also a DNA-binding motif proposed to play a role in the cross-talk between synthesis and degradation (33).

Stabilization of the primer-terminus at the 3′–5′ exonuclease of φ29 DNA polymerase. Primer-terminus transference between polymerization and exonuclease active sites

φ29 DNA polymerase mutant L567A showed a very reduced exonuclease activity on ssDNA substrates directly related to deficient ssDNA stabilization at its exonuclease active site. A strong ssDNA-binding reduction has been also reported for mutants T15I, at the conserved Thr15 of the Exo I motif (26), and F65S at the nearly invariant Phe65 belonging to the Exo II motif (27). In addition, and as described previously for mutant N62D at the invariant Asn residue of the Exo II motif, also shown to be essential for primer-terminus stabilization at the 3′–5′ exonuclease active site (26), substitution of Leu567 into Ala aborted the degradation of substrates shorter than 6/7mer. The 3′–5′ exonuclease activity defects displayed by mutant L567A were even more evident when such an activity was assayed on a template–primer structure. Under these conditions the binding strength at the exonuclease active site is not high enough to outcompete the primer stabilization at the polymerization active site, which is contributed by the enzyme itself and by Watson and Crick pairing. A direct consequence was the increased value of relative polymerization obtained with mutant L567A (4-fold), that lead to a 13-fold increase in the incidence of stable misincorporation. The biochemical characterization of mutant L567A, presented here, demonstrates the importance of Leu567 in the primer-terminus stabilization at the 3′–5′ exonuclease active site.

The role of residue Lys555 was also studied by the biochemical analysis of mutant K555A. Such a mutant derivative showed a 2.3-fold reduction in its exonuclease activity on dsDNA and a Pol/Exo ratio 2-fold higher than that of the wild-type enzyme, leading to a 4-fold decrease of its misincorporation fidelity. In this case, the reduced exonuclease activity could not be related to a defective ssDNA-binding stability at the 3′–5′ exonuclease active site. Modelling of the DNA from the structure of the RB69 DNA ternary complex (12) onto φ29 DNA polymerase shows that the side chain of Lys555 is very close and facing towards the primer strand, near the polymerization active site. Based on this placement and on the biochemical results obtained with mutant K555A, two possibilities are raised. On the one hand, Lys555 could be playing a role in triggering the switching of the primer-terminus between both active sites to remove, by the proofreading activity of the DNA polymerase, a misinserted nucleotide to preserve the fidelity of the replication process. On the other hand, it could be playing a role in orienting the primer-terminus correctly at the exonuclease active site, without contributing to the general binding stability.

In contrast, although mutant Q560A showed a reduction of its exonuclease activity on dsDNA similar to mutant K555A, it did not lead to an increase of its Pol/Exo ratio. This fact, together with its reduced binding stability on both ss- and dsDNA could suggest a role for residue Gln560 in primer interactions in both polymerization and editing modes, similarly to primer-terminus ligands reported to be present in the thumb subdomain of other crystallized DNA polymerases belonging to both family A and B (6,7,9,12). Structural analysis of polymerization versus editing complexes of those DNA polymerases show the thumb as the main subdomain involved in transferring the primer-terminus between both active sites during proofreading. The tip of the thumb maintains contacts with the phosphates of the primer strand in both polymerization and editing modes, by virtue of a thumb tip microdomain rotation towards the polymerization and the exonuclease sites, respectively, the base of the thumb staying in roughly the same orientation. The unusual φ29 DNA polymerase thumb subdomain does not present structurally differentiated microdomains (19). It is small, mainly made of a long β-turn-β element whose tip part buries the ssDNA, forming one wall of the ssDNA-binding cleft at the 3′–5′ exonuclease active site. This fact allows residue Leu567 to be faced toward and interacting with the two 3′-terminal bases of the ssDNA, in good agreement with the defective ssDNA-binding stability displayed by mutant L567A. Leu567, together with residues Thr15, Asn62 and Phe65 would form the ssDNA-binding core responsible of the stabilization of the 3′ end of the primer during the proofreading activity. In the crystallized φ29 DNA polymerase/oligo (dT)$_5$ complex, the thumb subdomain is predicted to be in an editing conformation, considering the appropriate location of Leu567 to interact with the ssDNA at the exonuclease site (19). Under these conditions, the thumb tip is also making contacts with the tip of the TPR2 insertion forming an arch expected to clamp the DNA during polymerization. In the absence of a complex with dsDNA, it could be predicted that, as in other DNA polymerases, upon substrate binding the thumb could adopt a more closed conformation, rotating down towards the palm to wrap around the primer–template substrate, allowing the thumb tip residues described above to interact with the primer-terminus at the polymerization active site. The absence of a flexible region between the tip and base parts of the thumb [in contrast to the flexible hinge between the tip and the base of the thumb subdomain of other crystallized DNA polymerases; (12)] could also indicate that either the thumb subdomain rotates as a whole or it does not rotate at all. If this last suggestion were the case, it would be tempting to speculate that the primer partitioning between both active sites in φ29 DNA polymerase could be accomplished by a

passive diffusion of the frayed primer-terminus from the polymerization to the exonuclease site, breaking specific interactions to stabilize the primer at the polymerization active site, creating new ones with residues specialized in binding the ssDNA at/towards the exonuclease active site, while other interactions would be kept all the time.

The DNA-binding role of the residues presented in this paper is in good agreement with the results obtained with a φ29 DNA polymerase deletion mutant lacking the C-terminal 13 residues. Such a derivative displayed a dramatically diminished affinity for both ss- and dsDNA substrates as a consequence of losing DNA ligands of the thumb subdomain (25). The presence of DNA-binding residues, specifically specialized in DNA stabilization either to one or both active sites, makes the thumb of φ29 DNA polymerase as the main subdomain responsible of the obliged communication between the synthetic and degradative activities during DNA replication, required to faithfully copy the genetic information.

ACKNOWLEDGEMENTS

Conflict of interest statement. None declared.

REFERENCES

1. Bebenek,K. and Kunkel,T.A. (2004) Functions of DNA polymerases. *Adv. Protein. Chem.*, **69**, 137–165.
2. Longley,M.J., Pierce,A.J. and Modrich,P. (1997) DNA polymerase delta is required for human mismatch repair *in vitro*. *J. Biol. Chem.*, **272**, 10917–10921.
3. Loeb,L.A. and Kunkel,T.A. (1982) Fidelity of DNA synthesis. *Annu. Rev. Biochem.*, **51**, 429–457.
4. Echols,H. and Goodman,M.F. (1991) Fidelity mechanisms in DNA replication. *Annu. Rev. Biochem.*, **60**, 477–511.
5. Kunkel,T.A. and Bebenek,K. (2000) DNA replication fidelity. *Annu. Rev. Biochem.*, **69**, 497–529.
6. Eom,S.H., Wang,J. and Steitz,T.A. (1996) Structure of *Taq* polymerase with DNA at the polymerase active site. *Nature*, **382**, 278–281.
7. Li,Y., Korolev,S. and Waksman,G. (1998) Crystal structures of open and closed forms of binary and ternary complexes of the large fragment of *Thermus aquaticus* DNA polymerase I: structural basis for nucleotide incorporation. *EMBO J.*, **17**, 7514–7525.
8. Wang,J., Sattar,A.K., Wang,C.C., Karam,J.D., Konigsberg,W.H. and Steitz,T.A. (1997) Crystal structure of a pol alpha family replication DNA polymerase from bacteriophage RB69. *Cell*, **89**, 1087–1099.
9. Doublie,S., Tabor,S., Long,A.M., Richardson,C.C. and Ellenberger,T. (1998) Crystal structure of a bacteriophage T7 DNA replication complex at 2.2 A resolution. *Nature*, **391**, 251–258.
10. Hopfner,K.P., Eichinger,A., Engh,R.A., Laue,F., Ankenbauer,W., Huber,R. and Angerer,B. (1999) Crystal structure of a thermostable type B DNA polymerase from *Thermococcus gorgonarius*. *Proc. Natl Acad. Sci. USA*, **96**, 3600–3605.
11. Rodriguez,A.C., Park,H.W., Mao,C. and Beese,L.S. (2000) Crystal structure of a pol alpha family DNA polymerase from the hyperthermophilic archaeon *Thermococcus sp.* 9 degrees N-7. *J. Mol. Biol.*, **299**, 447–462.
12. Franklin,M.C., Wang,J. and Steitz,T.A. (2001) Structure of the replicating complex of a pol alpha family DNA polymerase. *Cell*, **105**, 657–667.
13. Salas,M. (1999) Mechanisms of initiation of linear DNA replication in prokaryotes. *Genet. Eng. (N Y)*, **21**, 159–171.
14. Salas,M. and de Vega,M. (2006) Recent advances in DNA virus replication. *Bacteriophage Protein-Primed DNA Replication.* Research Signpost Transworld Research Network. In press.
15. Blanco,L., Bernad,A., Lazaro,J.M., Martin,G., Garmendia,C. and Salas,M. (1989) Highly efficient DNA synthesis by the phage phi 29 DNA polymerase. Symmetrical mode of DNA replication. *J. Biol. Chem.*, **264**, 8935–8940.
16. Garmendia,C., Bernad,A., Esteban,J.A., Blanco,L. and Salas,M. (1992) The bacteriophage phi 29 DNA polymerase, a proofreading enzyme. *J. Biol. Chem.*, **267**, 2594–2599.
17. Blanco,L. and Salas,M. (1995) Mutational analysis of bacteriophage phi 29 DNA polymerase. *Meth. Enzymol.*, **262**, 283–294.
18. Blanco,L. and Salas,M. (1996) Relating structure to function in phi29 DNA polymerase. *J. Biol. Chem.*, **271**, 8509–8512.
19. Kamtekar,S., Berman,A.J., Wang,J., Lazaro,J.M., de Vega,M., Blanco,L., Salas,M. and Steitz,T.A. (2004) Insights into strand displacement and processivity from the crystal structure of the protein-primed DNA polymerase of bacteriophage phi29. *Mol. Cell.*, **16**, 609–618.
20. Rodriguez,I., Lazaro,J.M., Blanco,L., Kamtekar,S., Berman,A.J., Wang,J., Steitz,T.A., Salas,M. and de Vega,M. (2005) A specific subdomain in phi29 DNA polymerase confers both processivity and strand-displacement capacity. *Proc. Natl Acad. Sci. USA*, **102**, 6407–6412.
21. Penalva,M.A. and Salas,M. (1982) Initiation of phage phi 29 DNA replication *in vitro*: formation of a covalent complex between the terminal protein, p3, and 5′-dAMP. *Proc. Natl Acad. Sci. USA*, **79**, 5522–5526.
22. Lazaro,J.M., Blanco,L. and Salas,M. (1995) Purification of bacteriophage phi 29 DNA polymerase. *Meth. Enzymol.*, **262**, 42–49.
23. Zaballos,A., Lazaro,J.M., Mendez,E., Mellado,R.P. and Salas,M. (1989) Effects of internal deletions on the priming activity of the phage phi 29 terminal protein. *Gene*, **83**, 187–195.
24. Carthew,R.W., Chodosh,L.A. and Sharp,P.A. (1985) An RNA polymerase II transcription factor binds to an upstream element in the adenovirus major late promoter. *Cell*, **43**, 439–448.
25. Truniger,V., Lazaro,J.M. and Salas,M. (2004) Function of the C-terminus of phi29 DNA polymerase in DNA and terminal protein binding. *Nucleic Acids Res.*, **32**, 361–370.
26. de Vega,M., Lazaro,J.M., Salas,M. and Blanco,L. (1996) Primer-terminus stabilization at the 3′–5′ exonuclease active site of phi29 DNA polymerase. Involvement of two amino acid residues highly conserved in proofreading DNA polymerases. *EMBO J.*, **15**, 1182–1192.
27. de Vega,M., Lazaro,J.M., Salas,M. and Blanco,L. (1998) Mutational analysis of phi29 DNA polymerase residues acting as ssDNA ligands for 3′–5′ exonucleolysis. *J. Mol. Biol.*, **279**, 807–822.
28. Bernad,A., Blanco,L., Lazaro,J.M., Martin,G. and Salas,M. (1989) A conserved 3′–5′ exonuclease active site in prokaryotic and eukaryotic DNA polymerases. *Cell*, **59**, 219–228.
29. Mendez,J., Blanco,L., Lazaro,J.M. and Salas,M. (1994) Primer-terminus stabilization at the psi 29 DNA polymerase active site. Mutational analysis of conserved motif TX2GR. *J. Biol. Chem.*, **269**, 30030–30038.
30. Blasco,M.A., Mendez,J., Lazaro,J.M., Blanco,L. and Salas,M. (1995) Primer terminus stabilization at the phi 29 DNA polymerase active site. Mutational analysis of conserved motif KXY. *J. Biol. Chem.*, **270**, 2735–2740.
31. Zhao,Y., Jeruzalmi,D., Moarefi,I., Leighton,L., Lasken,R. and Kuriyan,J. (1999) Crystal structure of an archaebacterial DNA polymerase. *Structure*, **7**, 1189–1199.
32. Dufour,E., Rodriguez,I., Lazaro,J.M., de Vega,M. and Salas,M. (2003) A conserved insertion in protein-primed DNA polymerases is involved in primer terminus stabilisation. *J. Mol. Biol.*, **331**, 781–794.
33. Truniger,V., Lazaro,J.M., Salas,M. and Blanco,L. (1996) A DNA binding motif coordinating synthesis and degradation in proofreading DNA polymerases. *EMBO J.*, **15**, 3430–3441.